

This article was downloaded by: [Tomsk State University of Control Systems and Radio]

On: 23 February 2013, At: 04:55

Publisher: Taylor & Francis

Informa Ltd Registered in England and Wales Registered Number: 1072954

Registered office: Mortimer House, 37-41 Mortimer Street, London W1T 3JH, UK



Molecular Crystals and Liquid Crystals

Publication details, including instructions for authors and subscription information:

<http://www.tandfonline.com/loi/gmcl16>

Supercooling and Nucleation in Liquid Crystals

D. Armitage^a & F. P. Price^b

^a Polymer Science and Engineering, University of Massachusetts, Amherst, MA, 01002

^b Liquid Crystal Institute, Kent State University, Kent, Ohio, 44242

Version of record first published: 19 Oct 2010.

To cite this article: D. Armitage & F. P. Price (1978): Supercooling and Nucleation in Liquid Crystals, *Molecular Crystals and Liquid Crystals*, 44:1-2, 33-44

To link to this article: <http://dx.doi.org/10.1080/00268947808084966>

PLEASE SCROLL DOWN FOR ARTICLE

Full terms and conditions of use: <http://www.tandfonline.com/page/terms-and-conditions>

This article may be used for research, teaching, and private study purposes. Any substantial or systematic reproduction, redistribution, reselling, loan, sub-licensing, systematic supply, or distribution in any form to anyone is expressly forbidden.

The publisher does not give any warranty express or implied or make any representation that the contents will be complete or accurate or up to date. The accuracy of any instructions, formulae, and drug doses should be independently verified with primary sources. The publisher shall not be liable for any loss, actions, claims, proceedings, demand, or costs or damages

whatsoever or howsoever caused arising directly or indirectly in connection with or arising out of the use of this material.

Supercooling and Nucleation in Liquid Crystals†

D. ARMITAGE‡ and F. P. PRICE§

Polymer Science and Engineering, University of Massachusetts, Amherst, MA 01002

(Received April 13, 1977)

A study of the supercooling of the isotropic to nematic transition in the homologous nematogens *p*-azoxyanisole (PAA) and heptyloxyazoxybenzene (HOAOB) is reported. Differential scanning calorimeter thermograms are consistent with a small supercooling $\sim 0.01^\circ\text{K}$. Observations of the nematic-isotropic phase boundary by optical microscopy reveals the development of a dendritic-like growth front with increasing rate of transformation to the nematic phase. This is also consistent with a supercooling $\sim 0.01^\circ\text{K}$. The boundary surfaces induce nematogenic alignment and therefore act as heterogeneous nucleation sites. Nucleation theory is used to show that if heterogeneous nucleation could be eliminated, the observable supercooling would be no more than $0.1(T_0 - T^*)$, where T_0 is the nematic-isotropic transition temperature and T^* is the pseudo-second order transition temperature.

INTRODUCTION

Liquid crystals in general undergo first order thermodynamic transitions but show some of the pretransition fluctuations characteristic of second order transitions.¹⁻³ First order transitions generally show supercooling behavior, while second order transitions being continuous in nature do not supercool.^{4,5} It is not obvious if liquid crystals should show supercooling in character with a first order nature, or whether the pretransition fluctuations will always nucleate the new phase.

We present some semiquantitative arguments and experimental results which indicate a small supercooling $\sim 0.01^\circ\text{K}$ is observable.

† Work supported by HEW grant 5 ROL HL 13188-07 BBCB.

‡ Present address: Liquid Crystal Institute, Kent State University, Kent, Ohio 44242.

§ With regret the untimely death of Professor F. P. Price is noted.

THEORY

A phase transition begins with the formation of nuclei of the new phase, which increase in number and volume, finally coalescing to complete the transition. Classical nucleation theory^{4,5} describes this process in terms of a volume and surface energy of the nuclei. A recognized limitation of this approach is the attribution of bulk properties to microscopic nuclei. Despite its obvious limitations, the classical approach produces sensible values for the physical parameters describing a wide variety of phase transitions. The classical result for spherical nuclei can be expressed:⁵ $J = \Omega \exp(-\Delta G/kT)$, where J is the nucleation rate, $\Omega = 10^{33 \pm 3} (\text{sec}^{-1} \text{cm}^{-3})$, $\Delta G = 17\sigma^3 T_0^2/H^2 \Delta T^2$, σ = surface energy, T_0 = transition temperature, H = transition enthalpy/cm³, ΔT = supercooling, and kT = Boltzmann energy. The nucleation temperature is usually⁵ taken as $J = 1 \text{ sec}^{-1} \text{cm}^{-3}$, where the arbitrariness of this assumption is mitigated by the extreme temperature dependence of J .

Substituting typical values¹⁻⁸ for *p*-azoxyanisole (PAA) (see materials section) and taking $\Omega = 10^{30}$ (to favor maximum supercooling) gives: for solid, $\Delta T = 25^\circ\text{K}$ and critical nucleus radius $r_c = 2\sigma T_0/H\Delta T = 30 \text{ \AA}$; for nematic, $\Delta T = 0.22^\circ\text{K}$, $r_c = 530 \text{ \AA}$. Since $\Delta T \sim \sigma^{1.5}$, the error in ΔT is about the same order as that of σ . The value of σ for PAA is not well established;^{6,8} however, it should not differ greatly from the reliable value of 0.02 erg/cm^2 for the well-known nematogen MBBA.^{3,9,10}

The elastic distortion energy of the bulk could be included. Approximating the bulk elastic energy of a sphere with tangential boundary¹¹ $E = 2\pi Kr$, this is found to be an important contribution of about the same magnitude as the surface energy. However, it is an overestimate since the continuum theory is not valid at these dimensions; moreover, the tangential boundary state would be sacrificed to lower the energy. A detailed treatment would show that a sphere is not the minimum energy shape of the nuclei when the anisotropic surface energy and bulk elastic properties are taken into account. We assume that all this can be accounted for by a small increase in the surface energy parameter σ in the spherical nucleus model.

An alternative approach is possible for mesophase transitions. Above the transition there exists short range order described¹⁻³ by a correlation function of the form $\exp(r/\xi)/r$, where the correlation length $\xi = \xi_0(T - T^*)^{-0.5}$ with $\xi \approx 100 \text{ \AA}$ at the transition point T_0 . The correlations would diverge at T^* and this provides an upper limit $\Delta T = T_0 - T^* \approx 1^\circ\text{K}$ for the supercooling.¹⁻³

A sophisticated version of the classical nucleation droplet model¹²⁻¹⁴ gives the droplet size distribution $N(r) = B \exp(-r^2/2\xi^2)/r^5$ where B is a temperature-independent constant that can be derived by making the crude approximation $N(\xi) \sim \xi^{-3}/\text{cm}^3$. Then for $N(r) = 1/\text{cm}^3$, $r = 800 \text{ \AA}$ if

$\xi \approx 100 \text{ \AA}$. The relaxation rate τ of such fluctuations should be about the same as for MBBA,^{1,15} which is of order $(r/\xi)^2 \mu \text{ sec}$; hence, about $6 \times 10^4/\text{sec cm}^3$ fluctuations with $r = 800 \text{ \AA}$ take place, well in excess of the $1/\text{sec cm}^3$ characteristic of the nucleation point. The result $r = 8\xi$ is insensitive to the approximation for B and τ on account of a logarithmic dependence. A weakness of this approach is that the validity of the correlation function at $r \gg \xi$ is not known. Assuming that classical volume and surface energetics determine the stability of this fluctuation, a supercooling $\Delta T = 0.1^\circ\text{K}$ can be deduced. Alternatively, if the exponential factor is identified with the energy of the fluctuation, viz. $r^2/2\xi^2 = E/kT$, then equating this to the volume term $4\pi r^3 \Delta TH/3T_0$ gives a supercooling $\Delta T = 0.02^\circ\text{K}$. In this approximation, $\Delta T \sim \xi^{-3}$ and to recover the earlier value $\Delta T = 0.2^\circ\text{K}$ requires $\xi = 50 \text{ \AA}$.

The supporting walls or even free surfaces will provide a preferred orientation, thus acting as heterogeneous nucleation sites.⁵ Heterogeneous nucleation always lowers the observable supercooling. Therefore, the ΔT which has been calculated on the basis of homogeneous nucleation is an upper limit to the observable value.

DIFFERENTIAL SCANNING CALORIMETRY

Since the DSC results are interpreted in an unorthodox way, a brief description is in order. We are specifically concerned¹⁶ with the Perkin-Elmer DSC 2, but the argument should be true for other instruments.¹⁷

The sample temperature is programmed to increase or decrease at a set rate and the heat required to do this is recorded. Since the heat flow requires a temperature gradient, it can be shown that the ideal delta function transition heat is recorded as a right triangle.^{16,17} This is easily seen in the thermogram of pure indium run at slow speed.

For a right triangle thermogram: width \sim peak height \sim (mass \times sweep rate)^{0.5}, which is easily verified using indium samples. It is of interest to note that the recorder deflection for specific heat \sim (mass)(sweep rate). Therefore to discriminate transition heat from specific heat favors a slow sweep, i.e., trans heat/sp. heat \sim (mass \times sweep rate)^{-0.5}.

The effect of supercooling on the thermogram can also be demonstrated with indium. A supercooled sample on crystallizing increases in temperature. The DSC control loop responds rapidly to this temperature jump. For indium the supercooled crystallization thermogram approximates a delta function. In general, on account of the temperature jump in a supercooled sample, the thermogram peak will be higher than that of the melting transition. Of course, if the crystal growth rate is low, this will limit the peak height. The ratio of peak heights can be used to infer supercooling.¹⁸

The best test of supercooling is obviously to measure the transition temperatures. There is on account of heat flow temperature gradients an inherent sweep-dependent error in temperature. This error changes in sign on cooling as opposed to heating. Using an indium sample, this error can be studied as a function of positive sweep rate, and we find the error $\delta T^{\circ}\text{K} = 0.035$ (sweep rate $^{\circ}\text{K}/\text{min}$). Assuming the magnitude of the error remains the same at negative sweep rates, the thermograms can be corrected for this error.

Equilibrium conditions can be approached by operating the DSC in a "step" mode. A minimum step of $\pm 0.1^{\circ}\text{K}$ can be made, the temperature remaining constant until such time as another step is triggered. The heat recorded during these step changes can be interpreted, but errors are introduced by the transient response of the instrument.

MATERIALS

P-azoxyanisole (PAA) obtained from Aldrich was purified by recrystallization from ethanol followed by zone refining.¹⁹ This technique is effective when the viscosity of the melt is low as in the nematic to solid transformation. The presence of a smectic to solid transformation generally requires special zone refining techniques.²⁰

Heptyloxyazoxybenzene (HOAOB) (Eastman) is the heptyl homologue of PAA and was purified by multiple recrystallizations from pentanol and then ethanol.

The DSC thermogram of the purified materials is as sharply defined as that of the pure DSC standards such as benzoic acid; therefore we estimate an upper impurity level $\sim 0.1\%$.

Samples are encapsulated in standard aluminum pans for the DSC, which is operated with nitrogen purge gas.

Relevant data: PAA, solid-nematic transition temperature $T_0 = 392^{\circ}\text{K}$, transition enthalpy $H = 105 \text{ J/ml}$, solid-nematic surface energy⁸ $\sigma = 10 \text{ erg/cm}^2$, nematic-isotropic $T_0 = 409^{\circ}\text{K}$, $H = 2.1 \text{ J/ml}$, surface^{6,8} $\sigma = 0.03 \text{ erg/cm}^2$; HOAOB, smectic-C to nematic 368.6°K , $H = 3.72 \text{ J/ml}$, nematic-isotropic 397.6°K , $H = 2.27 \text{ J/ml}$.

RESULTS

DSC

DSC thermograms were recorded for various PAA samples using the Perkin-Elmer DSC 2. Figure 1 shows the thermograms for a purified sample.

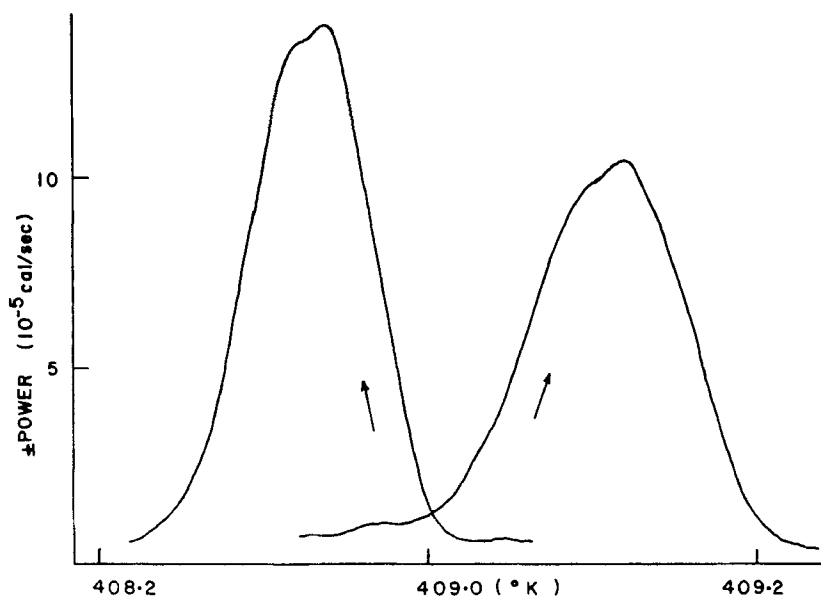


FIGURE 1 *P*-azoxyanisole DSC endotherm and exotherm (2 mg sample, 0.31°K/min).

The endotherm and exotherm are shown without distinguishing the sign of heat flow. The temperatures are corrected for machine hysteresis as discussed earlier. It is clear that the transitions begin at virtually the same temperatures. A small sample fails to conform to the ideal right triangle shape due to limiting sensitivity of the machine and sample transition range.

The effect of stepping through the transition is shown in Figure 2. Spikes result at each step due to the machine transient. However, most of the transition takes place in the step 409.0 to 409.1°K as indicated by the broader spike. This suggests as expected that the DSC exaggerates the transition width.

Returning to Figure 1 we note that the peak height of the exotherm is greater than that of the endotherm. As discussed earlier, this is indicative of supercooling. An estimate of the supercooling can be made according to $\Delta T = (\% \text{ increase in peak height}) (\text{half width}) = 0.03^\circ\text{K}$. It may also be accounted for by different thermal conductivities in nematic and isotropic phases. If that were the explanation the effect would be expected to increase with sample size or sweep speed. However, the opposite is observed. A sample pan of pure copper weighing 500 mg was substituted for the 20 mg aluminum pan that is normally used. This thermal inertia should inhibit any small temperature jump the sample might make at the transition. No significant change in the thermogram is observed with this procedure. This suggests that if there is a temperature jump it is confined to a temperature

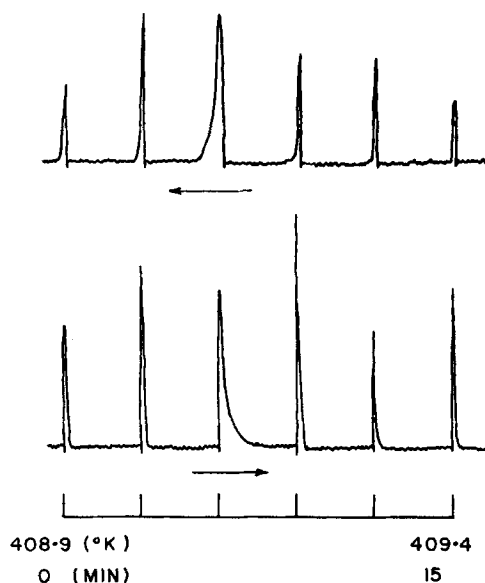


FIGURE 2 *P*-azoxyanisole DSC response to step changes 0.1°K at 3 min intervals.

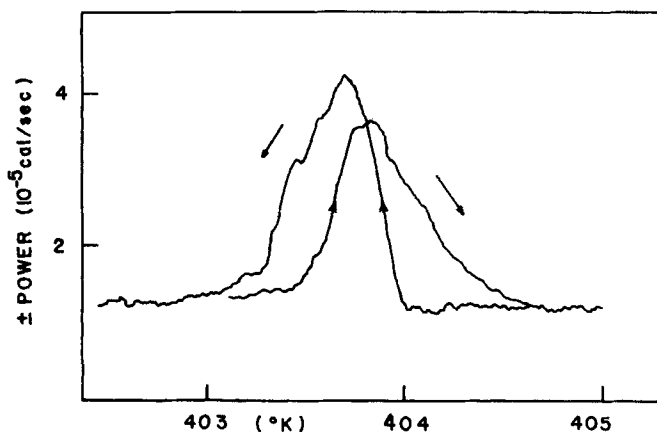


FIGURE 3 *P*-azoxyanisole DSC of impure sample. ($0.31^{\circ}\text{K}/\text{min}$).

gradient in the sample. There is some confirmation of this from observations on a sample mixed with 10μ glass powder where the two peaks are almost the same. The glass will, however, change the nucleation behavior as well as increase the thermal inertia.

Figure 3 shows the thermogram of an impure sample. The transitions are broader and overlap. There is a gap between the termination of the endotherm

and the start of the exotherm of about 0.5°K . This is expected on account of the higher solubility of impurities in the isotropic phase which gives rise to an impurity segregation in the two-phase region.

The experiments were repeated with HOAOB. The difference between isotropic exotherm and endotherm peaks is less than half the effect in PAA and corresponds to a supercooling 0.01°K .

Microscopy

Microscopic studies are carried out with a Zeiss polarizing microscope and FP4 Mettler hot stage. The birefringent nematic phase is easily distinguished from the isotropic phase during microscopic observation of the phase transition. Here, as is well known,²¹ we see the formation of nematic spherical droplets in the isotropic phase at the transition point. This is indicative of a nucleation process.⁵

A study of the phase boundary region is aided by the introduction of a temperature gradient such as to stabilize that region. This can be achieved in the Mettler hot stage by replacing the transparent heat shield with plain glass, thus producing a circular region of slightly lower temperature. Figure 4 shows how a nematic region about 1 mm diameter surrounded by isotropic

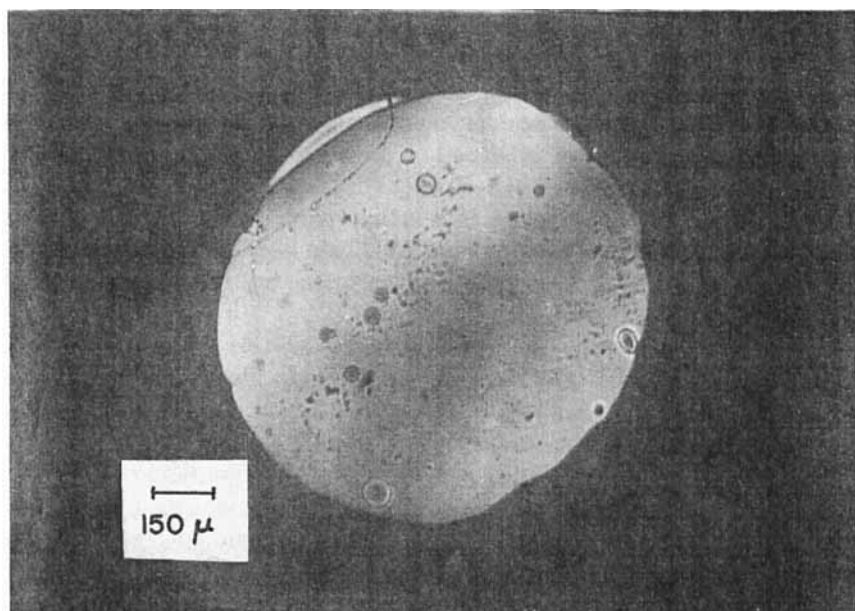


FIGURE 4 Photomicrograph of PAA in cleaved mica wedge showing nematic region surrounded by isotropic.

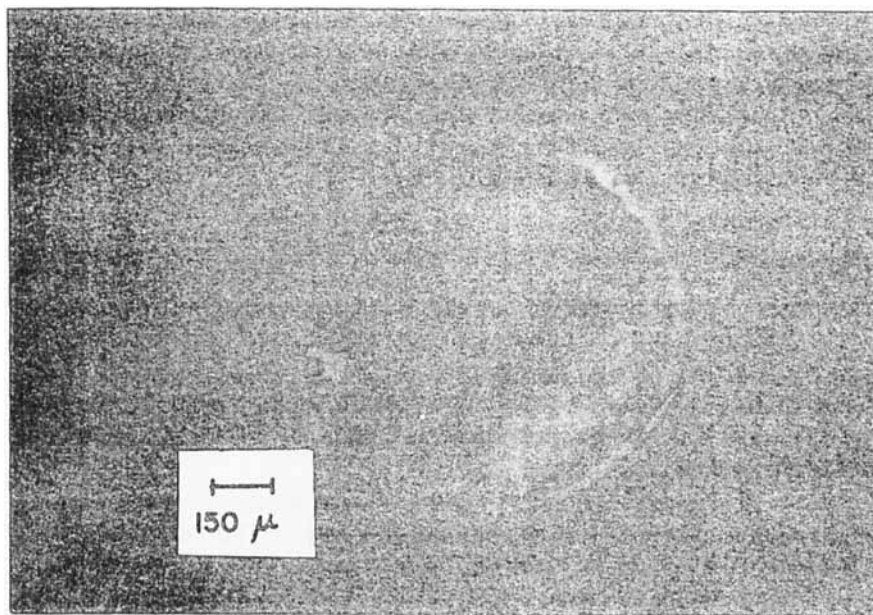


FIGURE 5 Sample shown in Figure 4, but moving 0.1 mm/sec. Movement produces dendritic growth front.

phase can be stabilized using this method. If the sample shown in Figure 4 is moved steadily through the temperature gradient an interesting growth pattern develops as shown in Figure 5. This looks like dendritic growth familiar from crystal growth experiments.²² Crystal growth rate increases with the degree of supercooling. The temperature at the growth front is raised by the heat of fusion and hence there is a non-uniform temperature distribution in the melt. This promotes an instability in the growth front favoring dendritic growth.

This effect is most easily seen with a thin film sample $\sim 1 \mu\text{m}$ in a freshly cleaved thin mica sheet. Alternatively the nematic film can be supported between thin cover glasses, the point being that the support should be of low thermal inertia to allow the temperature to change rapidly.

The width of the growth fringes decreases with the film thickness. This is ascertained by experiments on wedge-shaped films as shown in Figure 6. Here light and dark optical interference bands run perpendicular to the wedge direction. These are consistent with decreasing film thickness at the smaller growth fringes. The interference bands are used to calculate the film thickness, which is estimated to vary from $0.2 \mu\text{m}$ to $0.5 \mu\text{m}$ over the diameter shown in Figure 6. The fringed growth front is preceded by a bright halo. This is due

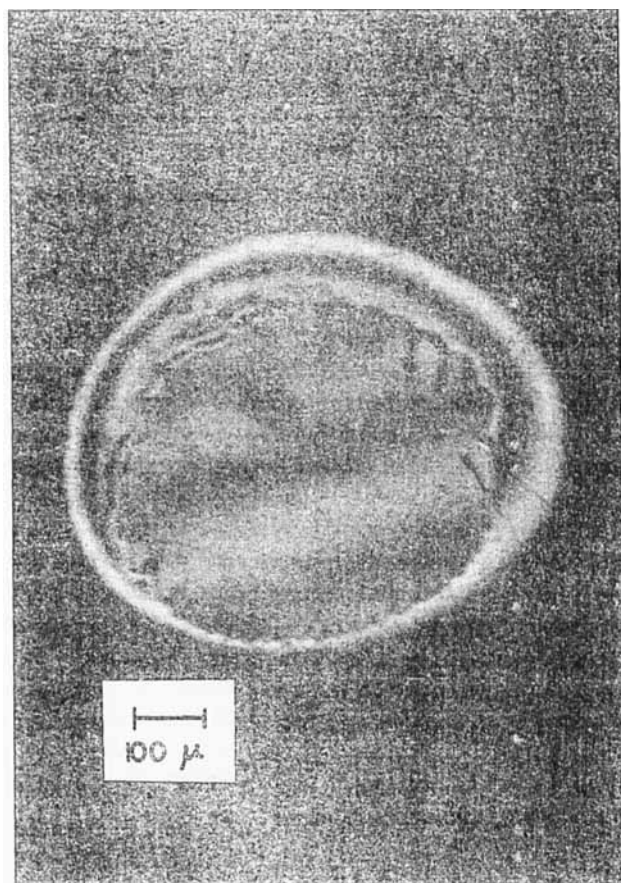


FIGURE 6 Similar to sample in Figure 5, but monochromatic light produces interference bands.

to a layer of nematic on one or both surfaces which does not yet extend through the sample thickness as shown in Figure 7, a conclusion that is reached from monochromatic studies such as Figure 6 which show “Newton ring” type interference behavior.

In these experiments the temperature difference between the disappearance of the nematic phase and the first appearance of the isotropic phase is checked by stepping the hot stage at 0.01°K intervals. A supercooling of about 0.03°K is found which is in agreement with the DSC results.

The growth fringes can naively be interpreted as manifestations of supercooling. An upper limit to the supercooling is estimated at 0.05°K from the maximum temperature difference observed in the hot stage.

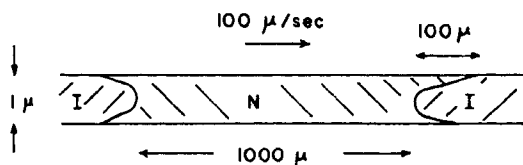


FIGURE 7 Cross section sketch of nematic-isotropic interface.

The dendrites propagate along the plane of the film at the expense of growth across the thickness of the film. This is favored by the curvature of the growth front as shown in Figure 7. A $1\text{ }\mu\text{m}$ radius cylindrical growth front concave to the nematic phase has an equilibrium temperature 0.006°K ($=\sigma T_0/rH$) higher than that of a plane interface. The dependence of growth fringe width on film thickness probably reflects the increased transition heat evolved in the thicker film. This requires a higher temperature gradient at the growth front, which is known to favor a coarser dendrite structure in crystals.²² The analogy with the growth of solid crystals may be misleading. A detailed interpretation of the phenomena will need to take into account: (1) supercooling, (2) heat flow and temperature distribution, (3) interfacial tension, (4) surface alignment properties, (5) elastic distortion energy, and (6) pressure changes induced by transition volume changes.

Similar experiments were performed with HOAOB. Here growth fringes are observed, but they are smaller and the effect seems much weaker. This is consistent with the DSC behavior. At the nematic-smectic transition an entirely different growth front is observed. This is in the form of a number of sharp spikes with no particular pattern.

DISCUSSION

The experiments demonstrate an apparent supercooling in PAA $\sim 0.01^\circ\text{K}$, which is in agreement with the value determined from droplet growth rate.²⁰ This is much less than the classically predicted value 0.2°K . The theoretical predictions are not firm; moreover, the experimentally determined value should be smaller on account of heterogeneous nucleation.

All of the containing surfaces have aligning properties, particularly mica. This aligned molecular surface layer should be preserved into the isotropic phase,^{2,3} and may therefore act as a nucleus when the sample is cooled to the nematic transition temperature. In this event the observations relate to the rate of transformation as a function of supercooling. A small decrease in temperature from the two-phase equilibrium will cause the nematic to grow by diffusive processes. However, rapid growth may require the nucleation

of a dendritic structure and necessitate supercooling to near the homogeneous nucleation temperature.

PAA shows the largest supercooling effect of several nematic and cholesteric materials.¹⁸ It is interesting to note that in the expression for correlation length $\xi = \xi_0(T_0 - T^*)^{-0.5}$, the upper limit of supercooling ($T_0 - T^*$) is comparatively high for PAA,²⁴⁻²⁸ i.e., for PAA,^{24,26} $T_0 - T^* = 3.0$ to 1.5°K , while for HOAOB^{24,25} $T_0 - T^* = 0.7$ to 0.6°K . This implies that supercooling should be more readily observed in PAA.

The value of $T_0 - T^*$ has been determined for several nematics²⁴⁻²⁷ and cholesterics²⁸ and is in the range 0.01 to 0.6°K . For these materials the asymmetry in the DSC peaks is much smaller than that of PAA.

Analysis of the pretransition behavior in terms of a second order transition approximation is usually curtailed about 1°K before the first order transition. It is argued that perturbations related to the first order point are significant close to the transition.¹⁻³ If our treatment of nucleation in nematics is valid, then it could be correct to treat the pretransition effect as "reliable" second order behavior up to the transition point, since the first order transition is precipitated by a statistically rare fluctuation.

Experiments on the size dependence of phase transitions using samples absorbed in porous silica⁸ can be related to the nucleation problem. A cylindrical pore of radius 600 \AA depresses the nematic-isotropic transition²⁹ $\Delta T = 0.1^\circ\text{K}$. With spherical geometry this should increase⁵ to $\Delta T = 0.2^\circ\text{K}$. The surface energy parameter derived from these experiments⁸ was used in the nucleation calculation, therefore guaranteeing the agreement $\Delta T = 0.2^\circ\text{K}$. The porous silica experiments⁸ introduce extra problems of interpretation in the nature of the silica-nematic interface. Nevertheless it appears improbable that supercoolings in excess of 0.2°K can be observed in PAA if some method of eliminating heterogeneous nucleation can be found.

The extrapolation of the pretransition correlations suggests an upper bound $\Delta T < T_0 - T^*$. This is significantly reduced when statistically rare fluctuations are considered. A reasonable limit appears to be $\Delta T < 0.1(T_0 - T^*)$.

References

1. P. G. de Gennes, *The Physics of Liquid Crystals* (Clarendon Press, Oxford, 1974).
2. M. J. Stephen and J. P. Straley, *Rev. Mod. Phys.* **46**, 617 (1974).
3. E. B. Priestley, P. J. Wojtowicz, and P. Sheng, *Introduction to Liquid Crystals* (Plenum Press, 1974).
4. A. R. Ubbelohde, *Melting and Crystal Structure* (Oxford University Press, 1965).
5. A. C. Zettlemoyer, editor, *Nucleation* (Dekker, New York, 1970).
6. W. R. Runyan and A. W. Nolle, *J. Chem. Phys.* **27**, 1081 (1957).
7. H. Arnold, *Z. Physik. Chem.* (Leipzig) **226**, 146 (1964).
8. D. Armitage and F. P. Price, *Chem. Phys. Lett.* **44**, 305 (1976).

9. D. Langevin and M. A. Bouchiat, *Mol. Cryst. Liq. Cryst.* **22**, 317 (1973).
10. R. Williams, *Mol. Cryst. Liq. Cryst.* **35**, 349 (1976).
11. E. duBois-Violette and O. Parodi, *J. de Phys.* **30**, C4-57 (1969).
12. M. E. Fisher, *Physics* (N.Y.) **3**, 255 (1967).
13. C. S. Kiang and D. Stauffer, *Z. Phys.* **235**, 130 (1970).
14. C. M. Sorenson, B. J. Ackerson, R. D. Mockler, and W. J. O'Sullivan, *Phys. Rev.* **A13**, 1593 (1976).
15. J. D. Litster and T. W. Stinson, III, *J. Appl. Phys.* **41**, 996 (1970).
16. Perkin-Elmer DSC II handbook.
17. E. M. Barrall, II and J. F. Johnson, *Liquid Crystals and Plastic Crystals*, v. 2, ed. by G. W. Gray and P. A. Winsor (Ellis Horwood, 1974).
18. D. Armitage and F. P. Price, *J. de Phys.* **36**, C1-133 (1975).
19. J. L. Habelfeld, E. C. Hsu, and J. F. Johnson, *Mol. Cryst. Liq. Cryst.* **24** (1973).
20. N. J. G. Bollin, M. J. Van Essen, and W. M. Smit, *Anal. Ch. Acta* **38**, 279 (1967).
21. W. Ostner, S. K. Chan, and M. Kahlweit, *Berichte der Bunsen-Gesellschaft für Phys. Chem.* **77**, 1122 (1973).
22. B. Chalmers, *Principles of Solidification* (John Wiley, N.Y., 1964).
23. G. W. Gray, *Molecular Structure and the Properties of Liquid Crystals* (Academic Press, London, 1962).
24. E. G. Hanson, Y. R. Shen, and G. K. L. Wong, *Phys. Rev.* **A14**, 1281 (1976).
25. D. Armitage and F. P. Price, *Phys. Rev.* **15**, 2069 (1977).
26. D. Armitage and F. P. Price, *Phys. Rev.* **15**, 2496 (1977).
27. D. Armitage and F. P. Price, *Mol. Cryst. Liq. Cryst.* **38**, 229 (1977).
28. D. Armitage and F. P. Price, *J. Chem. Phys.* **66**, 3414, (1977).
29. D. Armitage and F. P. Price, unpublished result.